IRIS AperTO

UNIVERSITÀ DEGLI STUDI DI TORINO

AperTO - Archivio Istituzionale Open Access dell'Università di Torino

HS-SPME-GCxGC-qMS volatile metabolite profiling of Chrysolina herbacea frass and Mentha spp. leaves

This is the author's manuscript

Original Citation:

Availability:

This version is available http://hdl.handle.net/2318/93120 since 2016-07-14T11:38:10Z

Published version:

DOI:10.1007/s00216-011-5600-4

Terms of use:

Open Access

Anyone can freely access the full text of works made available as "Open Access". Works made available under a Creative Commons license can be used according to the terms and conditions of said license. Use of all other works requires consent of the right holder (author or publisher) if not exempted from copyright protection by the applicable law.

(Article begins on next page)

16 September 2026

UNIVERSITÀ DEGLI STUDI DI TORINO

***This is an author version of the contribution published on**:*
Questa è la versione dell'autore dell'opera:
[Chiara Cordero, Simon Atsbaha Zebelo, Giorgio Gnavi, Alessandra Griglione, Carlo Bicchi, Massimo E. Maffei, Patrizia Rubiolo

ANALYTICAL AND BIOANALYTICAL CHEMISTRY Volume: 402 Issue: 9 Pages: 3017-3018 Published: MAR 2012, DOI 10.1007/s00216-011-5600-4]

The definitive version is available at:
La versione definitiva è disponibile alla URL:
[http://link.springer.com/article/10.1007/s00216-011-5600-4#page-2]

HS-SPME-GCxGC-qMS volatile metabolite profiling of *Chrysolina herbacea* frass and *Mentha* spp. leaves

Chiara Cordero[1a], Simon Atsbaha Zebelo[2a], Giorgio Gnavi[2], Alessandra Griglione[1], Carlo Bicchi[1], Massimo E. Maffei[2] and Patrizia Rubiolo [1*]

[1] Dipartimento di Scienza e Tecnologia del Farmaco, Università di Torino, Via Pietro Giuria n°9 - 10125 Torino, Italy

[2] Unità di Fisiologia Vegetale, Dipartimento di Biologia Vegetale, Università di Torino, Centro della Innovazione, Via Quarello 11/A, 10135 Torino, Italy

* Corresponding author

Prof. Dr. Patrizia Rubiolo

Dipartimento di Scienza e Tecnologia del Farmaco, Università degli Studi di Torino, Via Pietro Giuria 9, Turin 10125, Italy; Fax: +39 011 6707687; e-mail: patrizia.rubiolo@unito.it;

website: www.phytoanalysis.unito.it

[a]: These authors contributed equally

Abstract

Headspace solid-phase microextraction (HS-SPME) comprehensive two-dimensional (2D) gas chromatography combined with quadrupole-mass spectrometry (GCxGC-qMS) with dedicated comparative data elaboration was applied to separate chemical patterns arising from the interaction between some *Mentha* species and the herbivore *Chrysolina herbacea*, also known as the mint bug. Upon feeding on different *Mentha* species (*M. spicata* L., *M. x piperita* L. and *M. longifolia* L.), *C. herbacea* produced frass (faeces) which were characterized by a typical volatile fraction. HS-SPME GCxGC-qMS analysis of the complex volatile fraction of both mint leaf and *C. herbacea* frass was submitted to advanced fingerprinting analysis of 2D chromatographic data. 1,8-Cineole, found in the leaves of all the *Mentha* species examined, was oxidized and *C. herbacea* frass yielded high rates of several hydroxy-1,8-cineoles, including 2α-hydroxy-, 3α-hydroxy-, 3β-hydroxy- and 9-hydroxy-1,8-cineole**.** Upon insect feeding, several unknown oxidized monoterpenes, a *p*-menthane diol and three unknown phenylpropanoids were also detected in the frass volatiles. In *M. longifolia*, the occurrence of the monoterpene piperitenone oxide was found to be toxic and associated with insect death. The results of this work show that high throughput techniques such as HS-SPME and GCxGC-qMS fingerprint analysis are ideal tools to analyze complex volatile matrices, and provide a sensitive method for the direct comparison and chemical visualization of plant and insect emitted volatile components.

Keywords: Plant-insect interaction; *Chrysolina herbacea*; *Mentha spicata* L.; *Mentha* x *piperita* L.; *Mentha longifolia* L.; Volatile fraction; HS-SPME-GC×GC-qMS; Fingerprint analysis.

Introduction

Analysis of compounds arising from multitrophic interactions among different living organisms requires the selection of sample preparation and analytical strategies suitable to give reliable results helpful to understanding the biological phenomenon. When dealing with organisms belonging to different kingdoms, multitrophic interactions generate a level of complexity that requires high throughput strategies able to provide information on both the identity and the absolute and/or relative abundance distribution of specific markers. This information has to be obtained from a representative and appropriate amount of sample matrix (depending on their concentration) after suitable separation (or isolation, when necessary) and detection.

Headspace solid-phase microextraction (HS-SPME) combined with comprehensive two-dimensional (2D) GC and quadrupole-mass spectrometry (GCxGC-qMS) with dedicated comparative data elaboration is particularly suitable to solving complex problems such as chemical patterns arising from multitrophic interactions. HS-SPME is a suitable sampling technique, because: a) it is easy to standardize and gives reliable profiles suitable for comparison; b) it affords the concentration of trace and minor components while minimizing possible artefacts formation and losses, frequently produced with conventional extraction procedures (e.g., solvent extraction); and c) it reduces sample manipulation to a minimum. Conversely, this technique can sometimes produce analyte discriminations due to the nature of the fibre, only partly compensated by the adoption of a multicomponent fibre coating, and, last but not least, might influence an effective direct quantitative comparison between plant and insect samples composition due to their highly different nature.

GCxGC-qMS is currently adopted as separation technique not only because of its high separation power and sensitivity but also for its ability to produce more widely distributed and rationalized peak patterns [1] for chemically correlated group of analytes. GCxGC peak patterns can be combined with novel advanced data mining methods able to delineate sample fingerprints, with different discrimination potential, and to locate compounds (known and unknown) comparatively important for differential analyses [2,3].

Data mining approaches aiming to elaborate GCxGC patterns are classified as “non-targeted” methods [4] enabling an effective cross-sample analysis to discover relevant chemical cues (such as compositional similarities or differences) from multiple samples. Non-targeted cross-sample analysis evaluates each and every constituent in each and every sample by generating characteristic *feature*(*s*) for each and every constituent [5]. Detector intensities and mass spectroscopic profiles (total and/or selected ion) were used as characteristic *features* since they indicate analyte abundance and provide information on the identity thus affording, during the comparative elaboration, the ability to match reliably the corresponding *features* of the same analyte in all samples.

An example illustrating the above considerations is the multitrophic interaction between *Mentha* species (family: Lamiaceae) and their specialist herbivore insects. These plants, which store defence secondary metabolites, pose apparent chemical barriers to potential herbivore colonists, and seem accessible to relatively few insect lineages, possibly pre-adapted by use of chemically similar or related host plants [6]. Insects may respond to plants by choosing different feeding sites, by altering their consumption rates or by induction of physiological/detoxification enzymes [7]. As some insects become adapted to plant metabolites, interactions between the two kingdoms occasionally lead to highly specific relationships, as in the case of some *Mentha* species and the herbivore *Chrysolina herbacea* (mint bug or mint beetle) [8]. This model is ideal to develop new sensitive methods of analytical and bioanalytical investigations aimed to reveal multiple markers and code the complexity of the interaction.

Previous studies have shown that *C. herbacea* is perfectly adapted to the blend of terpenoids emitted by undamaged *Mentha aquatica* and uses this blend as a cue to locate the plants, while the plant was found to respond to herbivory with the modulation of terpenoid biosynthesis and gene expression and production of specific deterrent molecules [9]. Furthermore, feeding by *C. herbacea* on *M. aquatica* was found to induce a significant increase of jasmonic acid (JA), JA precursor, *cis*-(+)-12-oxophytodienoic acid (OPDA), and JA conjugate, (3*R*,7*S*)-jasmonoyl-L-isoleucine (JA-Ile), in *M. aquatica* leaves [10].

An open question is how insects tolerate or detoxify the high amount of terpenoids ingested and catabolise/biotransform them during the digestive process. To shed light on this topic, *C. herbacea* was fed with fresh leaves of three mints species characterized by different blends of volatile monoterpenoids: *M. spicata* L., characterized by carvone [11], *M.* x *piperita* L., containing menthol and menthone [12], and a chemotype of *M. longifolia* L., especially rich in piperitenone oxide [13].

The volatile fraction composition of the insect frass was also investigated and compared to that of intact leaves. Several significant variables were taken in consideration, including a) the low amounts of frass produced by each insect, necessitating several insects to collect a few milligrams of frass in order to obtain a workable sample, and b) the different nature of frass (semi-liquid) and leaves (solid). Therefore, peak patterns from leaves and frass samples were compared to ~~extract~~ obtain information on *feature* relative abundance (semi-quantitative differences); the procedure consisted of a preliminary screening for relevant *features*, to detect qualitative differences between sample patterns, by a *visual comparison* method [1], followed by a more comprehensive approach , to focus the more relevant chemical differences (known as *Comprehensive Template Matching Fingerprinting* [3]

The aim of this work was to develop a highly sensitive and direct comparative analysis method to reveal volatile metabolites emitted by *C. herbacea* frass as a function of *Mentha spp.* fed leaf volatiles in order to assess the ability of the insect to feed on plant toxic compounds and to study the role of frass volatiles from an ecological viewpoint.

Experimental

Plant material and growth conditions

M. spicata L., *M.* x *piperita* L. and *M. longifolia* L. were identified by Prof. Massimo Maffei and a voucher specimen of each species is deposited at the *Herbarium Taurinensis* of the Department of

Plant Biology, University of Turin. Stolons of *M. spicata, M.* x *piperita,* and *M. longifolia* were surface sterilized with 70% ethanol (Sigma-Aldrich, St. Louis, MO, USA) for 20 s, with sodium hypochlorite (1% v/v available chlorine) (Sigma-Aldrich) for 5 min, and were rinsed three times with sterile distilled water. Plants were grown in plastic pots with sterilized peat and vermiculite (v/v 4:1) at 23°C and 60% humidity using daylight fluorescent tubes at 270 μE m^{-2} s^{-1} with a photophase of 16 h and were used in all assay before full bloom.

Insect collection and rearing

Adults of *C. herbacea* (Duftschmid 1825) (order: Coleoptera, family: Chrysomelidae, subfamily: Chrysomelinae) were collected by hand from infested mint fields in the Turin province area. After collection, beetles were reared at 22^{o}C in ventilated glass chambers and fed with *M. spicata* L.*, M. x piperita L.* and *M. longifolia* five-node cuttings.

Leaf and frass HS-SPME sampling

Intact leaves (about 50 mg) from living plants of *Mentha* species were carefully picked-off immediately before the analysis and gently placed in hermetically sealed 2.0 mL vials for HS-SPME sampling. Frass fluid collected from insects feeding on *Mentha* species suitable to produce a 3-5 mg sample were transferred to a 2.0 mL headspace vials, weighed and hermetically sealed before HS-SPME sampling. A different phase ratio in sampling leaves and frass was applied in order to obtain an indication, although highly approximate, of the relative component abundance in the two matrices.

The SPME sampling device, containing divinylbenzene/carboxen/polydimethylsiloxane (DVB/CAR/PDMS) df 50/30 μm, 2 cm length fibre, was manually inserted into the sealed vial and the fibre exposed to the matrix headspace volatiles for 20 min at room temperature.

Control over consistency of performance for SPME was obtained by the equilibrium in-fibre internal standardization procedure [14, 15] The Internal Standard loading onto the SPME device was as follows: the SPME device was manually inserted into a 20 mL sealed vial containing 2 mL of ultra-pure water to which 2 µL of α-thujone (ISTD) standard working solution at 7.0 µg/mL was added. α-Thujone is known to be absent in mint volatile fraction [ref]. The fibre was exposed to the headspace at room temperature for 20 min, followed by exposure to the frass headspace for a second time for 20 min at room temperature.

Instrumentation

GCxGC analyses were carried out on an Agilent 6890 GC unit coupled to an Agilent 5975 MS detector operating in EI mode at 70 eV (Agilent Technologies, Little Falls, DE, USA). The transfer line was set at 270°C while the ion source temperature was set at 230°C. A "Standard Tune" option was used. The Full Scan acquisition was set at m/z 35-250, with the fast scanning option applied (10000 amu/s). The system was provided with a two-stage thermal modulator (KT 2004 loop modulator, Zoex Corporation, Houston, TX, USA) cooled with liquid nitrogen and with the hot jet pulse time set at 400 ms with modulation times of 4 s and 5 s. The hot-jet temperature programme was: from 160°C to 250°C at 3°C/min. Data were acquired by Agilent MSD ChemStation software (ver D.02.00.275) (Agilent Technologies, Little Falls, DE, USA) and processed using GC Image software (ver 2.1b0) (GC Image, LLC Lincoln NE, USA).

GCxGC-qMS operating conditions

GCxGC column set consisted of a ^{1}D SE52 column (95% polydimethylsiloxane, 5% phenyl) (30 m x 0.25 mm ID, 0.25 µm df) coupled with a ^{2}D OV1701 column (86% polydimethylsiloxane, 7%

phenyl, 7% cyanopropyl) (1 m x 0.1 mm ID, 0.10 μm df) (MEGA, Legnano , Italy) with a loop dimension of 1.0 m.

One microlitre of the *n*-alkanes standard solution at 10 ng/μL (*n*-C9 to *n*-C25) (Sigma-Aldrich, Milan, Italy) was automatically injected into the GC with an Agilent ALS 7683B injection system (injector: split/splitless; mode: split; split ratio: 1/100; temperature: 280°C). The HS-SPME sampled analytes were recovered through thermal desorption of the fibre for 10 min directly into the GC injector [injector: split/splitless; mode: split; split ratio: 1/10; temperature: 250°C; carrier gas: helium; flow mode: constant flow; flow rate: 1.0 mL/min (initial head pressure 280 KPa); temperature program: 45°C (1 min) to 260°C (5 min) at 2.5°C/min; modulation period: 4 s].

Volatiles were identified by comparing their linear retention indices (I^T_S) to those reported in an in-house database, a commercially available database [16] or from literature [17], and by comparing EI-MS fragmentation pattern similarity with compounds collected in commercial and in-house databases or, when available, with authentic standard confirmation. An Identity Spectrum Match factor above 850 resulting from the NIST Identity Spectrum Search algorithm (NIST MS Search 2.0) was determined to be acceptable for positive identification. MW information is also reported for those analytes where it was possible to recognize at least the molecular weight (MW) and/or a diagnostic fragmentation pattern, referred to a known skeleton reasonably derived from bio-transformation of plant secondary metabolites.. All compounds whose standards were not available in the authors' laboratory, were indicated in Table 1 as tentatively identified with an asterisk. Unknown mass spectra are shown in supplementary file S1.

Data elaboration

Comparative Visualization of GCxGC sample patterns.

The Comparative Visualization procedure was adopted for the preliminary processing of 2D chromatograms to locate *features* that indicate differences in volatiles composition between leaf and frass samples. This approach is an extension of conventional image-comparison techniques, such as side-by-side and flicker between images [18], and consists of metadata subtraction of a *sample* (or *analyzed*) 2D-chromatogram from a *reference* to reveal quali-quantitative differences in analytes distribution. GCxGC raw data can be represented as an a [m, n] matrix where a is the analyzed chromatogram with indexed pixels, and m is the ^{1}D and n the ^{2}D retention-time corresponding to the detector response, generating a three dimensional image assigned to each pixel. For a correct and reliable visual comparison, corresponding peaks from 2D chromatogram pairs are properly aligned and normalized in terms of response [19].

In the first step, one of the chromatograms is transformed into the retention-times plane to minimize the mean-square misalignment of the reliable peaks. Affine transformations (with scaling, translation, and shearing) were used to find the best fit between the peak pattern in the *reference* image and detected peaks in the *analyzed* chromatogram. After alignment, pairs can be visually inspected to reveal compositional differences.

In the visual comparison a *colorized fuzzy difference* visualization is applied, which uses the Hue-Intensity-Saturation (HIS) colorspace to color each pixel in the retention-times plane. The method first computes the difference at each data point. The pixel hue is set to green when the difference is positive and red when it is negative. The pixel intensity is set to the largest of the two values. The pixel saturation is set to the magnitude of the difference between the data points. Peaks are visible because large-valued data points yield bright pixels and small-valued data points yield dark pixels. If the difference is large, the color is saturated with red or green (depending on the largest data point); if the difference is small, the colour saturation is low, producing a grey level from black to white depending on intensity. Peaks with large differences therefore appear red or green and peaks with small differences appear white or grey. The fuzzy difference is computed as the difference between a data point and a small region of data points in the other chromatogram divided by the

largest of the two values in computing the saturation. Thus, the colors are saturated with red or green only when the relative difference rather than the absolute difference is large. Differences are evidenced by white circles that indicate *features* to be investigated as potential bio-transformation and/or degradation products. Numbers in Figure 1 correspond to the compounds in Table 1.

Comprehensive Template Matching Fingerprinting

The high number of apparent differences required a fingerprinting method to evaluate the most significant differences and to catalogue them comprehensively.

An advanced, effective and reliable non-targeted analysis approach known as *Comprehensive Template Matching Fingerprinting* [2,20] was adopted for a comprehensive comparative analysis of 2D chromatographic data and to correctly interpret visual differences. This method considers as comparative *feature*, each individual 2D peak together with its time coordinates, detector response and MS fragmentation pattern, and includes it in a *sample template* that can be used to compare plots directly and comprehensively. The method implies that a) a template is created by recording retention times, detector responses, and MS fragmentation patterns of the 2D peaks from a *source* chromatogram; b) the template is compared to the peak pattern of the next sample (*analyzed* chromatogram) in the set, to establish correspondences between peaks of the same analyte; c) the template is eventually transformed in the retention-times plane to compensate for retention times shifts; d) positive matches are confirmed through their retention time coherence and mass spectroscopic match factors (NIST algorithm similarity or identity); and e) peaks in the analyzed chromatogram without correspondences are added to the template and the “up-dated” template adopted for the further comparative steps. This procedure is applied to the entire set of sample chromatograms, to generate a *consensus template* of non-targeted peaks to adopt for the cross comparison of samples.

Results

One of the major challenges posed by multitrophic interactions is the discrimination of chemical patterns produced by the interacting organisms. The chemical patterns and their contribution to metabolic interactions between *Mentha* species and *C. herbacea* were analysed in attempt to elucidate these multitrophic interactions.

As a first step, the comparative visualizations of the volatile fractions of (*a*) *M. spicata, (b*) *M. x piperita* and (*c*) *M. longifolia* leaf volatiles (*reference* image) vs. the corresponding *C. herbacea* frass volatile fraction was evaluated (Figure 1). Plots were obtained by comparing volatile patterns of *frass* samples (*analyzed* chromatogram) to those of the leaves of mint species (*reference* chromatogram) picked from living plants after chromatogram scaling and normalization. An average number of 10-14 features were highlighted for *M. spicata* (Figure 1a) and *M. piperita* (Figure 1b) enabling the next investigation step implying, where possible, the identification of the corresponding 2D-peaks and/or the extraction of retention data and MS fragmentation pattern for unknown analytes. *M. longifolia* results required dedicated considerations; few differences were detectable between the leaf-frass chromatograms pair, as revealed by the visual comparison (Figure 1c). The colorized fuzzy ratio visualization shows that leaves produced a more intense chromatogram than frass; i.e., several *reference* image volatiles (red 2D peaks) are represented over the 2D plane while only few *analyzed* image peaks (green spots) referred to highly abundant analytes in the frass sample are reported. In addition, *C. herbacea* bugs stopped feeding and eventually died after a few hours of feeding on *M. longifolia* leaves, probably due to the presence of leaf toxic compounds.

Consensus template peak list obtained by applying the *Comprehensive Template Matching* procedure on 2D-chromatograms of *M. spicata, M. x piperita* and *M. longifolia* leaves used to feed *C. herbacea* and the corresponding frass volatile fraction are listed in Table 1. Each un-targeted peak is reported with its compound name (when identified), ^{1}D and ^{2}D retention times, linear retention indices (I^{T}_{S}), the normalized 2D volumes and the percent response, i.e., 2D Peak Volume

percentage (PV%) estimated on the Total Ion Current signal. The identification of each compound was considered reliable when a coherence of linear retention indices, mass spectra similarity and co-injection of an authentic standard was verified.

As expected, the major component of *M. spicata* was carvone and the main components of *M. x piperita* were menthol and menthone, whereas the main component of *M. longifolia* was piperitenone oxide (Table 1). The comprehensive peak list was then elaborated in view of the comparative visualization results by focusing the attention on those 2D-peaks (formerly defined *features*) that varied greatly, in terms of relative abundance (2D PV %) from leaf to frass and vice versa. Structure formulae of some significant compounds are reported in Fig. 2.

The distribution of the most informative *features* revealed in frass samples, obtained from bugs feeding on *M. spicata* (Fig. 3a), *M. x piperita* (Fig. 3b) and *M. longifolia* (Fig.3c), not present in the volatiles pattern from leaves (left side) and those revealed in leaf samples only are depicted in Figure 3. Variations are represented as the difference between 2D PV % from frass to leaf.

Several new compounds were found in the frass volatile fraction from *M. spicata*. Most of these were oxidation products of plants terpenoids (e.g., 1,8-cineole and its 2α-hydroxy, 3α-hydroxy and 9-hydroxy derivatives), acetylation products (e.g., *neo*-dihydrocarvyl acetate and *iso*-dihydrocarvyl acetate) and an unknown oxidized monoterpenoid (MW152 II). Many leaf volatiles were not found in the frass volatiles, including several green leaf volatiles and three sesquiterpene hydrocarbons (Figure 3a and Table 1). The content of all other leaf volatiles was reduced in the frass volatile fraction (Table 1).

The insect frass volatile fraction resulting from *M. x piperita* presented significant variation with neo-menthol, carvone, three unknown monoterpenes, three 1,8-cineole hydroxylated derivatives (2α-hydroxy, 3β-hydroxy and 9-hydroxy), a *p*-menthane diol and three unknown phenylpropanoids (Figure 3b and Table 1). Some terpenoids originally present in the leaf fraction were probably metabolized by the insect; among them α-terpineol and a series of sesquiterpene hydrocarbons

(Figure 3b and Table 1). The amount of most of the remaining leaf compounds were decreased in the frass volatile fraction (Table 1).

A few compounds were found in the frass volatiles derived from *M. longifolia*, among these two alkanals, two monoterpenes and two hydroxylated cineole derivatives (Figure 3c and Table 1). Most of the major leaf volatiles were not present in the frass volatile fraction (Figure 3c and Table 1) while other leaf components (e.g., α- and β-pinene, sabinene and myrcene) increased in the frass compared to the leaves. (Table 1). Spectroscopic data of unknown *Mentha spp.* volatiles are provided as Supplementary Data S1.

Discussion

The set of techniques here applied successfully contributed to clarify the volatile variations when *C. herbacea* feeds on some *Mentha* species. Advanced fingerprinting procedures (i.e., comparative visualization and *Comprehensive Template Matching*) revealed informative *features* from a complex GC×GC-qMS data-set [1,3]. In particular, their potentials to provide further and specific discrimination between leaf volatiles of different mint species and *C. herbacea* frass was assessed.

Specifically, HS-SPME in combination with GCxGC-qMS allowed the study of the volatile fraction composition of *C. herbacea* frass, and the comparison of the obtained results to those of fed species belonging to the *Mentha* genus to investigate the possible metabolic transformation. Moreover, the comparative approach based on differential pattern visualization allowed us: a) to run qualitative analysis (based on retention time location over the Euclidean 2D-plane) and evaluate compound abundance based on detector intensity/response; b) to obtain information on differential sample composition, leaving out chemical identifications; and c) to monitor simultaneously several related or unrelated biological markers. Furthermore, the ability of *C. herbacea* to metabolize many leaf volatile terpenoids (e.g., those present in *M. spicata* and *M. x piperita*) producing new compounds, most of them being oxygenated derivatives of leaf volatiles was shown.

1,8-Cineole (eucalyptol) oxidation was found to occur in all plant species considered in this work. This compound is one of the common components of essential oils from *Mentha* species [21] and shows a significant bioactivity as a mosquito feeding deterrent, ovipositional repellent and toxicant against stored-grain beetles [22]. Oxidation of 1,8-cineole resulted in high rates of several hydroxy-1,8-cineoles [23]. 3-Hydroxycineole, the α- and β-isomers, have been reported as metabolites of the commonly occurring 1,8-cineole, arising from either animal, insect or microbial biotransformation [17,24]. Many insects feeding on plants that store 1,8-cineole are able to metabolize it into several hydroxyl-derivatives [17,25]. For example, faeces of grasshoppers feeding on the Lamiaceae *Pityrodia jamesii* contain a mixture of hydroxycineoles, of which 3α-hydroxy-1,8-cineole is the predominant isomer [26]. Southwell and co-workers [17] were the first to raise the question of whether the function of 1,8-cineole hydroxylation was detoxification or metabolism for the production of semiochemicals. Possums [27], Leichhardt's grasshopper [26] and perhaps the pyrgo beetle [28] have been proposed to use hydroxycineoles as pheromonal markers. This is also a possibility for *C. herbacea,* and a study is under way in this respect.

The monoterpenoids carvone and *Z*-carveol were detected in *C. herbacea* frass after feeding on *M. x. piperita*, a mint species that does not contain these two terpenes but accumulates limonene [29]. Several microorganism have been found to transform limonene to *Z*-carveol and carvone [30-33]. For example, *Rhodococcus opacus* PWD4 cells hydroxylated limonene at position 6 forming enantiomerically pure carveol, while *R. globerus* PWD8 catalyzed its conversion into carvone [34]. Since microorganisms possess metabolic properties that are absent in insects they may act as "microbial brokers," enabling phytophagous insects to overcome biochemical barriers to herbivory [35,36]. Thus, microbial degradation of plant toxic compounds can occur in insect guts and contribute to the carbon and energy requirement of the host [37]. A current study on *C. herbacea* microbial population revealed the presence of more than 200 bacterial isolates from the insect digestive tract, with most of the species showing ability to biotransform terpenoids (Atsbaha et al., unpublished).

Feeding on *M. longifolia* was found to cause death of *C. herbacea*. The main constituent of this mint is piperitenone oxide, which has been found to be highly active (LC_{50}: 9.95 mg l^{-1}) when screened on the insect *Culex pipiens* larvae [38] and on the root-knot nematode *Meloidogyne* sp. [39]. The toxicity of piperitenone oxide is one of the possible explanations of the inability of *C. herbacea* to feed on *M. longifolia* and justifies the low rate of leaf terpenoid conversion found in the frass volatile fraction.

Conclusions

The strategy and the techniques here adopted have been shown to be effective to discriminate terpenoids transformed by the digestive process of insect herbivores from molecules stored in the secretory tissues of fed plants. These techniques can therefore lead to discovery of new compounds and metabolites with specific structures, thus contributing to better understanding of the ecology and phytochemistry of plant-insect interactions. High throughput techniques such as HS-SPME and GCxGC-qM can be used as reliable tools to analyze complex volatile matrixes like those generated by plant-insect interactions.

Acknowledgements

This work was partly supported by the Doctorate School of Pharmaceutical and Biomolecular Sciences of the University of Turin.

Appendix A. Supplementary data

Supplementary data associated with this article can be found as Supplementary Data S1

References

1. Cordero C, Bicchi C, Rubiolo P (2008) Group-type and fingerprint analysis of roasted food matrices (coffee and hazelnut samples) by comprehensive two-dimensional gas chromatography. J Agric Food Chem 56:7655-7666

2. Cordero C, Liberto E, Bicchi C, Rubiolo P, Reichenbach SE, Tian X, Tao QP (2010) Targeted and non-Targeted approaches for complex natural sample profiling by GCxGC-qMS. J Chromatogr Sci 48:251-261

3. Cordero C, Liberto E, Bicchi C, Rubiolo P, Schieberle P, Reichenbach SE, Tao QP (2010) Profiling food volatiles by comprehensive two-dimensional gas chromatography coupled with mass spectrometry: Advanced fingerprinting approaches for comparative analysis of the volatile fraction of roasted hazelnuts (*Corylus avellana* L.) from different origins. J Chromatogr A 1217:5848-5858

4. Pierce KM, Hoggard JC, Mohler RE, Synovec RE (2008) Recent advancements in comprehensive two-dimensional separations with chemometrics. J Chromatogr A 1184:341-352

5. Reichenbach S, Tian X, Cordero C, Tao QP (2011) , Features for non-targeted cross-sample analysis with comprehensive two-dimensional chromatography. J Chromatogr A, In press doi:10.1016/j.chroma.2011.07.046].

6. Farrell BD, Mitter C (1994) Adaptive radiation in insects and plants - time and opportunity. Am Zool 34:57-69

7. Scriber JM (2002) Evolution of insect-plant relationships: chemical constraints, coadaptation, and concordance of insect/plant traits. Entomol Exp Appl 104:217-235

8. Bienkowski AO (2009) Feeding behavior of leaf-beetles (*Coleoptera, Chrysomelidae*). Zool Z 88:1471-1480

9. Zebelo SA, Bertea CM, Bossi S, Occhipinti A, Gnavi G, Maffei ME (2010) *Chrysolina herbacea* modulates terpenoid biosynthesis of *Mentha aquatica* L. Plos One 6

10. Occhipinti A, Zebelo SA, Capuzzo A, Maffei M, Gnavi G (2011) *Chrysolina herbacea* modulates jasmonic acid, cis-(+)-12-oxophytodienoic acid, (3R,7S)-jasmonoyl-l-isoleucine, and salicylic acid of local and systemic leaves in the host plant *Mentha aquatica*. J Plant Interact 6:99-101

11. Lawrence BM (2007) Mint: The genus *Mentha*. CRC Press edn., Boca Raton, FL

12. Maffei M, Sacco T (1987) Chemical and morphometrical comparison between 2 peppermint notomorphs. Planta Med:214-216

13. Maffei M (1988) A chemotype of *Mentha longifolia* (L.) Hudson particularly rich in piperitenone oxide. Flav Fragr J 3:23-26

14. Wang YX, O'Reilly J, Chen Y, Pawliszyn J (2005) Equilibrium in-fibre standardisation technique for solid-phase microextraction. J Chromatogr A 1072:13-17

15. Setkova L, Risticevic S, Linton CM, Ouyang G, Bragg LM, Pawliszyn J (2007) Solid-phase microextraction-gas chromatography-time-of-flight mass spectrometry utilized for the evaluation of the new-generation super elastic fiber assemblies. Anal Chim Acta 581:221-231

16. Adams R (2001) Identification of essential oil component by gas chromatography/quadrupole mass spectroscopy. Allured Publishing Corporation, Carol Stream, IL

17. Southwell IA, Russell MF, Maddox CDA, Wheeler GS (2003) Differential metabolism of 1,8-cineole in insects. J Chem Ecol 29:83-94

18. Lemkin P, Merril C, Lipkin L, Van Keuren M, Oertel W, Shapiro B, Wade M, Schultz M, Smith E (1979) Software aids for the analysis of 2D gel electrophoresis images. Comput Biomed Res 12:517-524

19. Hollingsworth BV, Reichenbach SE, Tao QP, Visvanathan A (2006) Comparative visualization for comprehensive two-dimensional gas chromatography. J Chromatogr A 1105:51-58

20. Reichenbach SE, Ni MT, Kottapalli V, Visvanathan A (2004) Information technologies for comprehensive two-dimensional gas chromatography. Chemom Intell Lab Syst 71:107-120

21. Croteau R, Alonso WR, Koepp AE, Johnson MA (1994) Biosynthesis of monoterpenes - partial-purification, characterization, and mechanism of action of 1,8-cineole synthase. Arch Biochem Biophys 309:184-192

22. ObengOfori D, Reichmuth CH, Bekele J, Hassanali A (1997) Biological activity of 1,8 cineole, a major component of essential oil of *Ocimum kenyense* (Ayobangira) against stored product beetles. J Appl Entomol 121:237-243

23. Duisken M, Sandner F, Blomeke B, Hollender J (2005) Metabolism of 1.8-cineole by human cytochrome P450 enzymes: Identification of a new hydroxylated metabolite. Biochim Biophys Acta-Gen Subj 1722:304-311

24. Carman RM, Robinson WT, Wallis CJ (2005) The 3-hydroxycineoles. Austr J Chem 58:785-791

25. Schmidt S, Walter GH, Moore CJ (2000) Host plant adaptations in myrtaceous-feeding Pergid sawflies: essential oils and the morphology and behaviour of *Pergagrapta l*arvae (Hymenoptera, Symphyta, Pergidae). Biol Linn Soc 70:15-26

26. Fletcher MT, Lowe LM, Kitching W, Konig WA (2000) Chemistry of Leichhardt's grasshopper, Petasida ephippigera, and its host plants, *Pityrodia jamesii, P-ternifolia*, and *P. pungens*. Journal of Chemical Ecology 26:2275-2290

27. Carman RM, Klika KD (1992) Partially racemic compounds as brushtail possum urinary metabolites. Austr J Chem 45:651-657

28. Southwell IA, Maddox CDA, Zalucki MP (1995) Metabolism of 1,8-cineole in tea tree (*Melaleuca-alternifolia* and *Melaleuca-linariifolia)* by pyrgo beetle (*Paropsisterna-tigrina*). Journal of Chemical Ecology 21:439-453

29. Maffei M, Chialva F, Sacco T (1989) Glandular trichomes and essential oils in developing peppermint leaves. New Phytol 111:707-716

30. Duetz WA, Fjallman AHM, Ren SY, Jourdat C, Witholt B (2001) Biotransformation of D-limonene to (+) trans-carveol by toluene-grown *Rhodococcus opacus* PWD4 cells. Appl Environ Microbiol 67:2829-2832

31. Krings U, Berger RG (2010) Terpene Bioconversion - How Does its Future Look? Nat Prod Comm 5:1507-1522

32. Duetz WA, Bouwmeester H, van Beilen JB, Witholt B (2003) Biotransformation of limonene by bacteria, fungi, yeasts, and plants. Appl Microbiol Biotechnol 61:269-277

33. Abraham WR, Hoffmann HMR, Kieslich K, Reng G, Stumpf B (1985) Microbial transformations of some monoterpenoids and sesquiterpenoids. Ciba Found Symp 111:146-160

34. Bicas JL, Fontanille P, Pastore GM, Larroche C (2008) Characterization of monoterpene biotransformation in two pseudomonads. J Appl Microbiol 105:1991-2001

35. Dillon RJ, Dillon VM (2004) The gut bacteria of insects: nonpathogenic interactions. Annu Rev Entomol 49:71-92

36. Shi WB, Syrenne R, Sun JZ, Yuan JS (2010) Molecular approaches to study the insect gut symbiotic microbiota at the 'omics' age. Insect Sci 17:199-219

37. Brune A, Miambi E, Breznak JA (1995) Roles of oxygen and the intestinal microflora in the metabolism of lignin-derived phenylpropanoids and other monoaromatic compounds by termites. Appl Environ Microbiol 61:2688-2695

38. Koliopoulos G, Pitarokili D, Kioulos E, Michaelakis A, Tzakou O (2010) Chemical composition and larvicidal evaluation of *Mentha, Salvia,* and *Melissa* essential oils against the West Nile virus mosquito *Culex pipiens*. Parasitol Res 107:327-335

39. Duschatzky CB, Martinez AN, Almeida NV, Bonivardo SL (2004) Nematicidal activity of the essential oils of several Argentina plants against the root-knot nematode. J Essent Oil Res 16:626-628

Legend for Figures

Fig. 1. Comparative visualization represented as colorized fuzzy ratio of leaf (reference image) vs. frass (analyzed image) from three different mint species: (a) *Mentha spicata*, (b) *Mentha x piperita*, (c) *Mentha longifolia*. Red colorization indicates 2D peaks more abundant in the reference image, while intense green peaks indicate those more abundant in the analyzed chromatogram. White circles indicate minutiae features to be investigated as potential bio-transformation and/or degradation products. Numbers correspond to compound numbers of Table 1.

Fig. 2. Terpenoids significantly characterizing the volatile fraction of leaves and frass. **1**, carvone; **2**, menthol; **3**, menthone; **4**, piperitenone oxide; **5**, 1,8-cineole; **6**, 2α-hydroxy-1,8-cineole; **7**, 3α-hydroxy-1,8-cineole; **8**, 9-hydroxy-1,8-cineole; **9**, 3β-hydroxy-1,8-cineole.

Fig. 3. Distribution of the main features revealed by the Comprehensive Template Matching fingerprinting for (**a**)*Mentha spicata*, (**b**) *Mentha piperita* and (**c**)*Mentha longifolia*. Variations are represented as the difference between 2D Peak Volumes % (PV%) from frass to leaf. The first group (left) collects compounds revealed in frass samples and not in leaves, the second (right) those revealed in the leaf volatiles profile only.

Table 1. *Consensus template* peak list from 2D-chromatograms fingerprinting of mint leaves and the corresponding frass samples collected after 30 minutes of air exposure. Each un-targeted peak is reported with its numbering (#ID), compound name (when identified), ^{1}D and ^{2}D Retention times, linear retention indexes (I^{T}_{S}), Normalized 2D Volume and the Peak Volume percentage (PV%). Data are the mean of three replicates. Boldface numbers indicate new compounds metabolized by *Chrysolina herbacea*. n.d. = not detected.

# ID	Compound Name	Peak I (min)	Peak II (s)	I^{T}_{S}	*Mentha spicata*				*Mentha x piperita*				*Mentha longifolia*			
					Leaf		Frass		Leaf		Frass		Leaf		Frass	
					Norm. Volume	PV %	Norm. Volume	PV %	Norm. Volume	PV %	Norm. Volume	PV %	Norm. Volume	PV %	Norm. Volume	PV %
1	*Z*-3-Hexenal	9.35	0.84	816	210.71	0.20	n.d.	n.d.	n.d.	n.d.	n.d.	n.d.	36.02	2.06	n.d.	n.d.
2	*E*-2-Hexenal	11.69	1.26	859	218.86	0.21	n.d.	n.d.	5.64	0.01	n.d.	n.d.	10.68	0.61	n.d.	n.d.
3	*E*-Hex-3-en-1-ol	11.75	1.64	860	1471.92	1.40	n.d.	n.d.	2.22	<0.01	7.24	0.05	3.11	0.18	n.d.	n.d.
4	*E*-2-Hexen-1-ol	12.29	1.56	870	82.95	0.08	n.d.	n.d.	67.98	0.08	5.10	0.04	98.35	5.62	n.d.	n.d.
5	α-Thujene	15.42	0.72	927	84.59	0.08	n.d.	n.d.	126.56	0.15	30.51	0.22	n.d.	n.d.	n.d.	n.d.
6	α-Pinene	15.75	0.76	933	1062.85	1.01	12.21	0.26	324.33	0.37	11.28	0.08	2.19	0.13	3.51	0.20
7	Camphene	16.62	0.80	949	16.40	0.02	n.d.	n.d.	5.59	0.01	n.d.	n.d.	n.d.	n.d.	n.d.	n.d.
8	β-Pinene	18.02	0.88	974	459.19	0.44	17.67	0.38	496.10	0.57	47.03	0.33	1.43	0.08	9.19	0.51
9	1-Octen-3-ol	18.22	1.60	978	54.95	0.05	n.d.	n.d.	36.45	0.04	n.d.	n.d.	n.d.	n.d.	n.d.	n.d.
10	Sabinene	18.22	0.88	978	995.12	0.95	7.19	0.15	275.20	0.32	75.11	0.53	2.60	0.15	5.12	0.29
11	Myrcene	18.89	0.93	990	836.17	0.80	16.85	0.36	69.43	0.08	16.39	0.12	2.21	0.13	9.70	0.54
12	3-Octanol	19.15	1.52	995	115.81	0.11	n.d.	n.d.	25.08	0.03	n.d.	n.d.	2.87	0.16	n.d.	n.d.
13	α-Phellandrene	19.49	0.84	1001	14.25	0.01	n.d.	n.d.	18.24	0.02	1.18	0.01	n.d.	n.d.	n.d.	n.d.
14	*E*-Hex-3-enyl acetate	19.82	1.30	1007	497.06	0.47	n.d.	n.d.	290.32	0.33	6.09	0.04	38.51	2.20	n.d.	n.d.
15	α-Terpinene	20.42	0.97	1017	26.54	0.03	n.d.	n.d.	66.52	0.08	5.82	0.04	n.d.	n.d.	n.d.	n.d.
16	*p*-Cymene	20.95	1.14	1027	33.43	0.03	7.82	0.17	96.25	0.11	14.58	0.10	4.22	0.24	1.67	0.09
17	Limonene	21.22	1.14	1031	14312.94	13.63	197.80	4.22	383.77	0.44	143.28	1.01	4.39	0.25	4.86	0.27
18	1,8-Cineole	21.29	1.09	1033	929.65	0.89	18.41	0.39	4003.42	4.59	127.99	0.91	13.40	0.76	n.d.	n.d.
19	*Z*-β-ocimene	22.22	1.01	1049	174.46	0.17	8.35	0.18	10.48	0.01	7.94	0.06	n.d.	n.d.	**6.51**	**0.36**
20	γ-Terpinene	22.75	1.05	1058	2.39	<0.01	1.56	0.03	114.26	0.13	10.57	0.07	n.d.	n.d.	n.d.	n.d.
21	*Z*-Sabinene hydrate	23.42	1.60	1070	12.57	0.01	n.d.	n.d.	944.95	1.08	77.38	0.55	n.d.	n.d.	n.d.	n.d.
22	α-Terpinolene	24.69	1.01	1092	78.61	0.07	n.d.	n.d.	51.77	0.06	5.59	0.04	n.d.	n.d.	n.d.	n.d.

# ID	Compound Name	Peak I (min)	Peak II (s)	I^T_S	*Mentha spicata*				*Mentha x piperita*				*Mentha longifolia*			
					Leaf		Frass		Leaf		Frass		Leaf		Frass	
					Norm. Volume	PV %	Norm. Volume	PV %	Norm. Volume	PV %	Norm. Volume	PV %	Norm. Volume	PV %	Norm. Volume	PV %
23	*p*-Cymenene	24.75	1.30	1093	55.72	0.05	10.03	0.21	5.46	0.01	14.59	0.10	n.d.	n.d.	n.d.	n.d.
24	2-Nonanol	25.02	1.56	1098	8.03	0.01	n.d.	n.d.	3.09	n.d.	n.d.	n.d.	n.d.	n.d.	n.d.	n.d.
25	Linalool	25.29	1.68	1102	142.88	0.14	n.d.	n.d.	273.12	0.31	8.14	0.06	n.d.	n.d.	n.d.	n.d.
26	Nonanal	25.55	1.52	1107	20.38	0.02	10.35	0.22	7.82	0.01	6.28	0.04	n.d.	n.d.	**4.68**	**0.26**
27	Allo-ocimene	27.02	1.18	1133	252.70	0.24	7.86	0.17	7.77	0.01	5.67	0.04	n.d.	n.d.	**4.73**	**0.26**
28	*Z*-Limonene oxide	27.35	1.43	1138	36.75	0.03	n.d.	n.d.	n.d.	n.d.	n.d.	n.d.	n.d.	n.d.	n.d.	n.d.
29	*E*-Limonene oxide	27.55	1.47	1142	80.57	0.08	n.d.	n.d.	n.d.	n.d.	n.d.	n.d.	n.d.	n.d.	n.d.	n.d.
30	Unknown monoterpene MW 152 I	27.55	1.30	1142	n.d.	n.d.	n.d.	n.d.	n.d.	n.d.	**66.39**	**0.47**	n.d.	n.d.	n.d.	n.d.
31	Unknown monoterpene MW 152 II	27.69	2.06	1144	n.d.	n.d.	**5.11**	**0.11**	18.68	0.02	274.52	1.94	n.d.	n.d.	n.d.	n.d.
32	Isopulegol	27.95	1.81	1149	n.d.	n.d.	n.d.	n.d.	76.47	0.09	17.45	0.12	n.d.	n.d.	n.d.	n.d.
33	Menthone	28.55	1.73	1159	5.44	0.01	n.d.	n.d.	14502.36	16.64	268.29	1.90	n.d.	n.d.	n.d.	n.d.
34	Menthofuran	29.09	1.39	1169	13.05	0.01	7.85	0.17	504.68	0.58	181.41	1.28	88.05	5.03	n.d.	n.d.
35	Isomenthone	29.15	1.77	1170	77.87	0.07	7.18	0.15	10641.47	12.21	1.86	0.01	n.d.	n.d.	n.d.	n.d.
36	Neo-menthol	29.49	1.89	1176	n.d.	n.d.	**10.22**	**0.22**	3.40	<0.01	611.00	4.32	n.d.	n.d.	n.d.	n.d.
37	Dill Ether	29.69	1.60	1179	n.d.	n.d.	n.d.	n.d.	n.d.	n.d.	**24.71**	**0.17**	n.d.	n.d.	n.d.	n.d.
38	Menthol	30.15	1.89	1187	n.d.	n.d.	n.d.	n.d.	22525.94	25.85	8449.77	59.77	10.60	0.61	5.21	0.29
39	Isomenthol	30.49	1.73	1193	n.d.	n.d.	n.d.	n.d.	337.05	0.39	69.13	0.49	n.d.	n.d.	n.d.	n.d.
40	α-Terpineol	30.69	1.85	1197	53.47	0.05	n.d.	n.d.	95.44	0.11	n.d.	n.d.	5.07	0.29	n.d.	n.d.
41	Neoiso-menthol	30.75	1.73	1198	n.d.	n.d.	n.d.	n.d.	29.52	0.03	16.70	0.12	n.d.	n.d.	n.d.	n.d.
42	Diidro-carveol	30.95	1.98	1201	951.88	0.91	72.83	1.55	n.d.	n.d.	n.d.	n.d.	n.d.	n.d.	n.d.	n.d.
43	Decanal	31.42	1.56	1210	15.03	0.01	11.68	0.25	22.07	0.03	13.39	0.09	n.d.	n.d.	**4.87**	**0.27**
44	*E*-Diidro-carvone	31.49	1.94	1211	90.87	0.01	95.66	2.04	n.d.	n.d.	n.d.	n.d.	n.d.	n.d.	n.d.	n.d.
45	4,7-Dimethyl benzofuran	31.89	1.85	1218	n.d.	n.d.	n.d.	n.d.	6.93	0.01	n.d.	n.d.	73.63	4.20	n.d.	n.d.
46	2α-Hydroxy-1,8-cineol	32.42	2.40	1228	n.d.	n.d.	**7.54**	**0.16**	n.d.	n.d.	**83.35**	**0.59**	n.d.	n.d.	**8.43**	**0.47**
47	*E*-Carveol	32.49	2.15	1229	1191.19	1.13	306.58	6.54	n.d.	n.d.	**4.67**	**0.03**	n.d.	n.d.	n.d.	n.d.
48	*Z*-Carveol	32.95	1.94	1238	8.30	0.01	18.69	0.40	n.d.	n.d.	n.d.	n.d.	n.d.	n.d.	n.d.	n.d.
49	*Z*-3-Hexenyl isovalerate	33.22	1.35	1243	106.19	0.10	4.54	0.10	10.34	0.01	6.11	0.04	n.d.	n.d.	**1.67**	**0.09**
50	3α-Hydroxy-1,8-cineol	33.35	2.53	1245	n.d.	n.d.	**15.66**	**0.33**	n.d.	n.d.	n.d.	n.d.	n.d.	n.d.	n.d.	n.d.

# ID	Compound Name	Peak I (min)	Peak II (s)	I^{T}_{S}	*Mentha spicata*				*Mentha x piperita*				*Mentha longifolia*			
					Leaf		Frass		Leaf		Frass		Leaf		Frass	
					Norm. Volume	PV %	Norm. Volume	PV %	Norm. Volume	PV %	Norm. Volume	PV %	Norm. Volume	PV %	Norm. Volume	PV %
51	Pulegone	33.49	1.85	1248	403.66	0.38	6.15	0.13	9.85	0.01	n.d.	n.d.	n.d.	n.d.	n.d.	n.d.
52	3β-Hydroxy-1,8-cineol	33.55	2.44	1249	n.d.	n.d.	n.d.	n.d.	n.d.	n.d.	**131.26**	**0.93**	n.d.	n.d.	n.d.	n.d.
53	Carvone	33.82	2.06	1254	57917.53	55.14	656.97	14.01	n.d.	n.d.	**386.74**	**2.74**	n.d.	n.d.	n.d.	n.d.
54	Piperitone	34.09	2.36	1259	n.d.	n.d.	n.d.	n.d.	605.32	0.69	38.04	0.27	n.d.	n.d.	**27.79**	**1.55**
55	9-Hydroxy-1,8-cineol	34.55	2.23	1267	n.d.	n.d.	**12.28**	**0.26**	n.d.	n.d.	**6.90**	**0.05**	n.d.	n.d.	**3.91**	**0.22**
56	Neo-menthylacetate	35.15	1.64	1278	n.d.	n.d.	n.d.	n.d.	59.59	0.07	6.95	0.05	n.d.	n.d.	n.d.	n.d.
57	Menthyl acetate	36.35	1.52	1300	3.41	<0.01	n.d.	n.d.	1.84	<0.01	134.44	0.95	n.d.	n.d.	n.d.	n.d.
58	Neo-dihydrocarvyl acetate	36.95	1.68	1312	n.d.	n.d.	**13.03**	**0.28**	n.d.	n.d.	n.d.	n.d.	n.d.	n.d.	n.d.	n.d.
59	Iso-dihydrocarvyl acetate	38.15	1.60	1335	3.90	<0.01	136.58	2.91	n.d.	n.d.	n.d.	n.d.	n.d.	n.d.	n.d.	n.d.
60	Unknown sesquiterpene MW 204	38.29	1.18	1337	11.83	0.01	n.d.	n.d.	2.54	<0.01	n.d.	n.d.	n.d.	n.d.	n.d.	n.d.
61	*E*-*p*-Menthane-2,3-diol	38.55	2.99	1342	n.d.	n.d.	n.d.	n.d.	n.d.	n.d.	**139.10**	**0.98**	n.d.	n.d.	n.d.	n.d.
62	*E*-Carvyl acetate	38.62	1.64	1344	18.57	0.02	7.41	0.16	n.d.	n.d.	n.d.	n.d.	n.d.	n.d.	n.d.	n.d.
63	Eugenol	39.35	2.48	1358	n.d.	n.d.	**29.56**	**0.63**	n.d.	n.d.	n.d.	n.d.	n.d.	n.d.	n.d.	n.d.
64	α-Cubebene	39.42	1.26	1359	113.36	0.11	n.d.	n.d.	58.88	0.07	n.d.	n.d.	n.d.	n.d.	n.d.	n.d.
65	Unknown MW 174	39.49	2.10	1360	281.66	0.27	n.d.	n.d.	n.d.	n.d.	**20.36**	**0.14**	n.d.	n.d.	n.d.	n.d.
66	Z-Carvyl acetate	39.95	1.68	1369	14.54	0.02	51.77	1.10	n.d.	n.d.	n.d.	n.d.	n.d.	n.d.	n.d.	n.d.
67	Unknown phenylpropanoid MW 148 I	40.02	3.16	1371	34.02	0.03	n.d.	n.d.	n.d.	n.d.	**20.73**	**0.15**	n.d.	n.d.	n.d.	n.d.
68	Piperitenone oxide	40.35	2.57	1377	n.d.	n.d.	n.d.	n.d.	n.d.	n.d.	n.d.	n.d.	366.73	20.94	n.d.	n.d.
69	α-Copaene	40.55	1.26	1381	61.36	0.06	n.d.	n.d.	59.42	0.07	n.d.	n.d.	n.d.	n.d.	n.d.	n.d.
70	β-Bourbonene	41.35	1.35	1396	1113.00	1.06	18.92	0.40	186.73	0.21	n.d.	n.d.	n.d.	n.d.	n.d.	n.d.
71	β-Elemene	41.62	1.39	1401	1552.61	1.48	18.77	0.40	213.86	0.25	n.d.	n.d.	n.d.	n.d.	n.d.	n.d.
72	Unknown phenylpropanoid MW 148 II	41.89	3.16	1407	63.29	0.06	n.d.	n.d.	n.d.	n.d.	**8.39**	**0.06**	n.d.	n.d.	n.d.	n.d.
73	*E*-Jasmone	41.89	2.31	1407	25.20	0.02	n.d.	n.d.	n.d.	n.d.	n.d.	n.d.	n.d.	n.d.	n.d.	n.d.
74	Unknown phenylpropanoid MW 148 III	42.15	3.28	1412	24.84	0.02	n.d.	n.d.	n.d.	n.d.	**9.40**	**0.07**	n.d.	n.d.	n.d.	n.d.
75	Unknown phenylpropanoid MW 148 IV	42.35	3.32	1416	101.78	0.10	n.d.	n.d.	n.d.	n.d.	**16.20**	**0.11**	n.d.	n.d.	n.d.	n.d.
76	α-Gurjunene	42.62	1.30	1422	74.79	0.07	n.d.	n.d.	75.66	0.09	n.d.	n.d.	n.d.	n.d.	n.d.	n.d.
77	β-Cariophyllene	43.15	1.52	1432	2689.85	2.56	23.36	0.50	4686.50	5.38	17.50	0.12	19.77	1.13	n.d.	n.d.
78	*E*-aromadendrene	43.89	1.39	1447	n.d.	n.d.	n.d.	n.d.	77.63	0.09	n.d.	n.d.	n.d.	n.d.	n.d.	n.d.

# ID	Compound Name	Peak I (min)	Peak II (s)	I^{T}_{S}	*Mentha spicata*				*Mentha x piperita*				*Mentha longifolia*			
					Leaf		Frass		Leaf		Frass		Leaf		Frass	
					Norm. Volume	PV %	Norm. Volume	PV %	Norm. Volume	PV %	Norm. Volume	PV %	Norm. Volume	PV %	Norm. Volume	PV %
79	α-Humulene	44.82	1.47	1466	382.06	0.36	5.13	0.11	301.64	0.35	n.d.	n.d.	n.d.	n.d.	n.d.	n.d.
80	α-Amorphene	45.89	1.39	1488	425.81	0.41	n.d.	n.d.	176.22	0.20	n.d.	n.d.	n.d.	n.d.	n.d.	n.d.
81	Germacrene D	46.22	1.60	1495	3064.95	2.92	9.11	0.19	1155.97	1.33	7.06	0.05	6.28	0.36	n.d.	n.d.
82	α-Muurolene	46.75	1.47	1506	331.00	0.32	n.d.	n.d.	145.76	0.17	n.d.	n.d.	n.d.	n.d.	n.d.	n.d.
83	Bicyclogermacrene	46.89	1.52	1509	440.83	0.42	2.98	0.06	462.00	0.53	n.d.	n.d.	n.d.	n.d.	n.d.	n.d.
84	γ-Cadinene	47.69	1.43	1526	419.80	0.40	5.45	0.12	220.56	0.25	n.d.	n.d.	3.33	0.19	n.d.	n.d.
85	δ-Cadinene	48.09	1.43	1534	552.14	0.53	6.34	0.14	330.15	0.38	7.08	0.05	4.22	0.24	n.d.	n.d.
86	Cadina-1,4-diene	48.55	1.47	1544	46.75	0.04	n.d.	n.d.	24.45	0.03	n.d.	n.d.	n.d.	n.d.	n.d.	n.d.
87	α-Cadinene	48.82	1.47	1550	200.35	0.19	n.d.	n.d.	89.85	0.10	n.d.	n.d.	n.d.	n.d.	n.d.	n.d.
88	*epi*-Cubenol	52.42	1.89	1627	51.78	0.05	10.43	0.22	n.d.	n.d.	n.d.	n.d.	n.d.	n.d.	n.d.	n.d.
89	α-Cadinol	53.55	1.98	1651	8.85	0.01	n.d.	n.d.	5.74	0.01	n.d.	n.d.	n.d.	n.d.	n.d.	n.d.

Figure 1

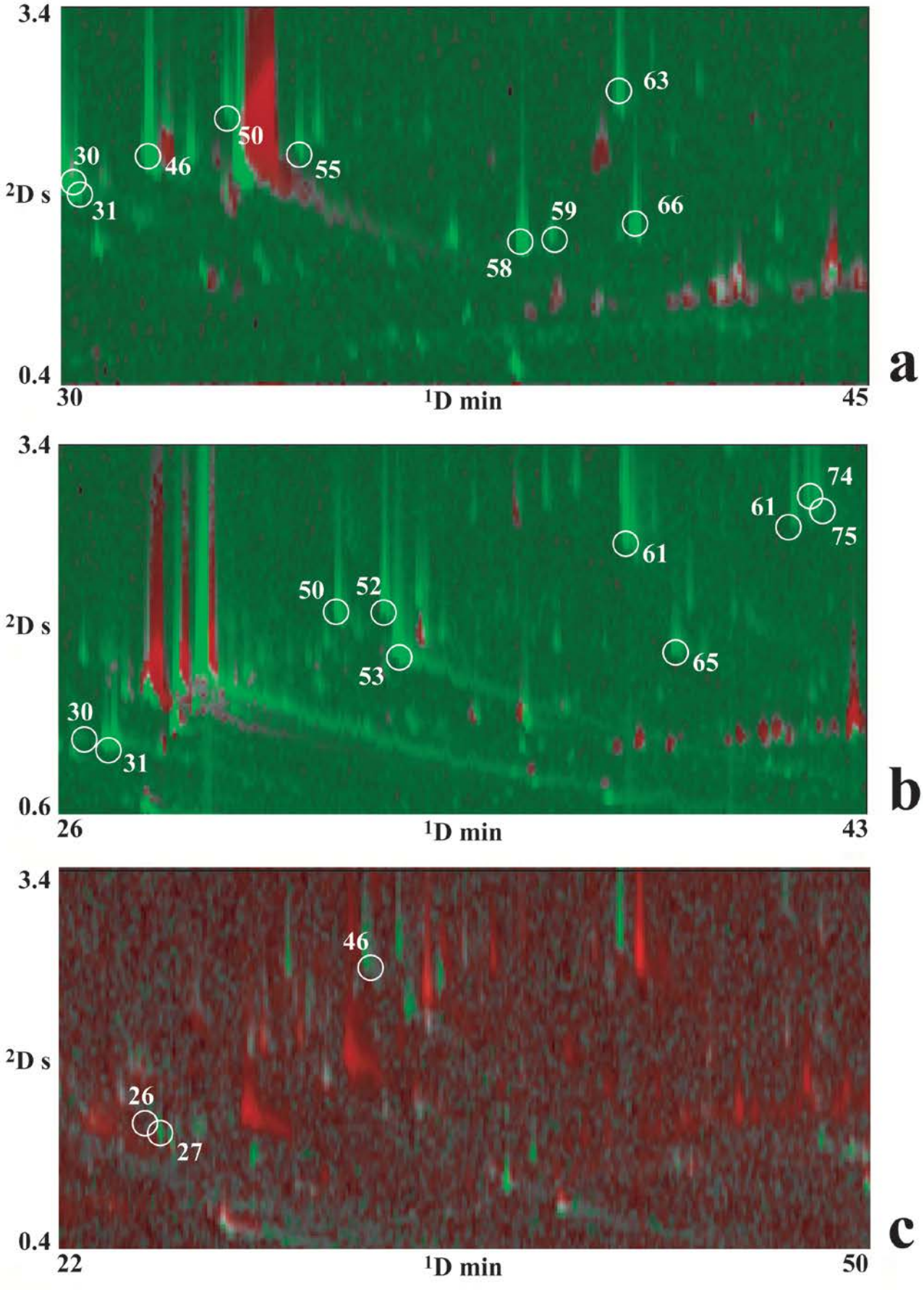
3.4
0.4
^{2}D s
30
^{1}D min
45
63
50
30
46
55
31
59
66
58
a
3.4
0.6
^{2}D s
26
^{1}D min
43
74
61
75
61
50
52
65
53
30
31
b
3.4
0.4
^{2}D s
22
^{1}D min
50
46
26
27
c

Figure 2

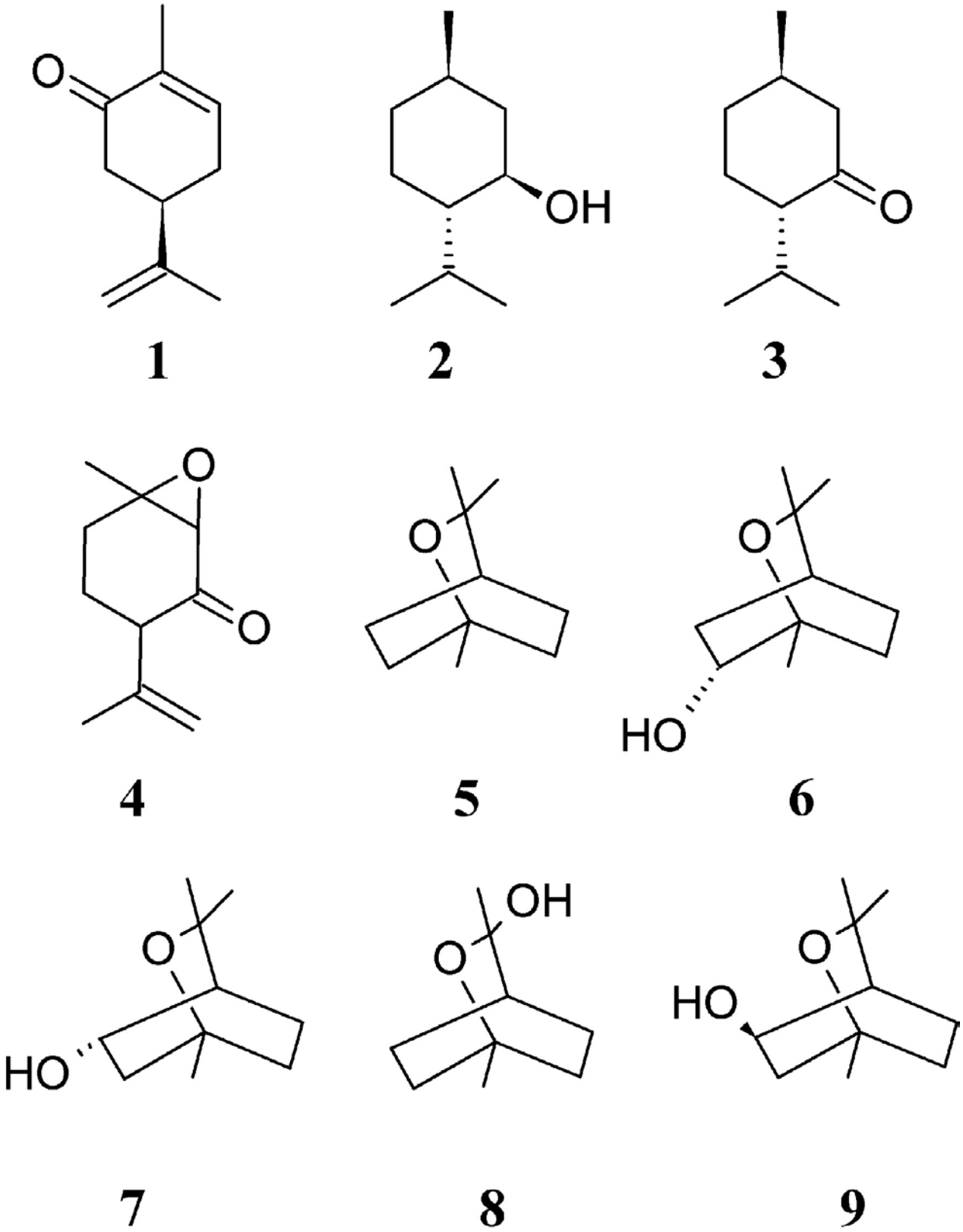

Figure 3

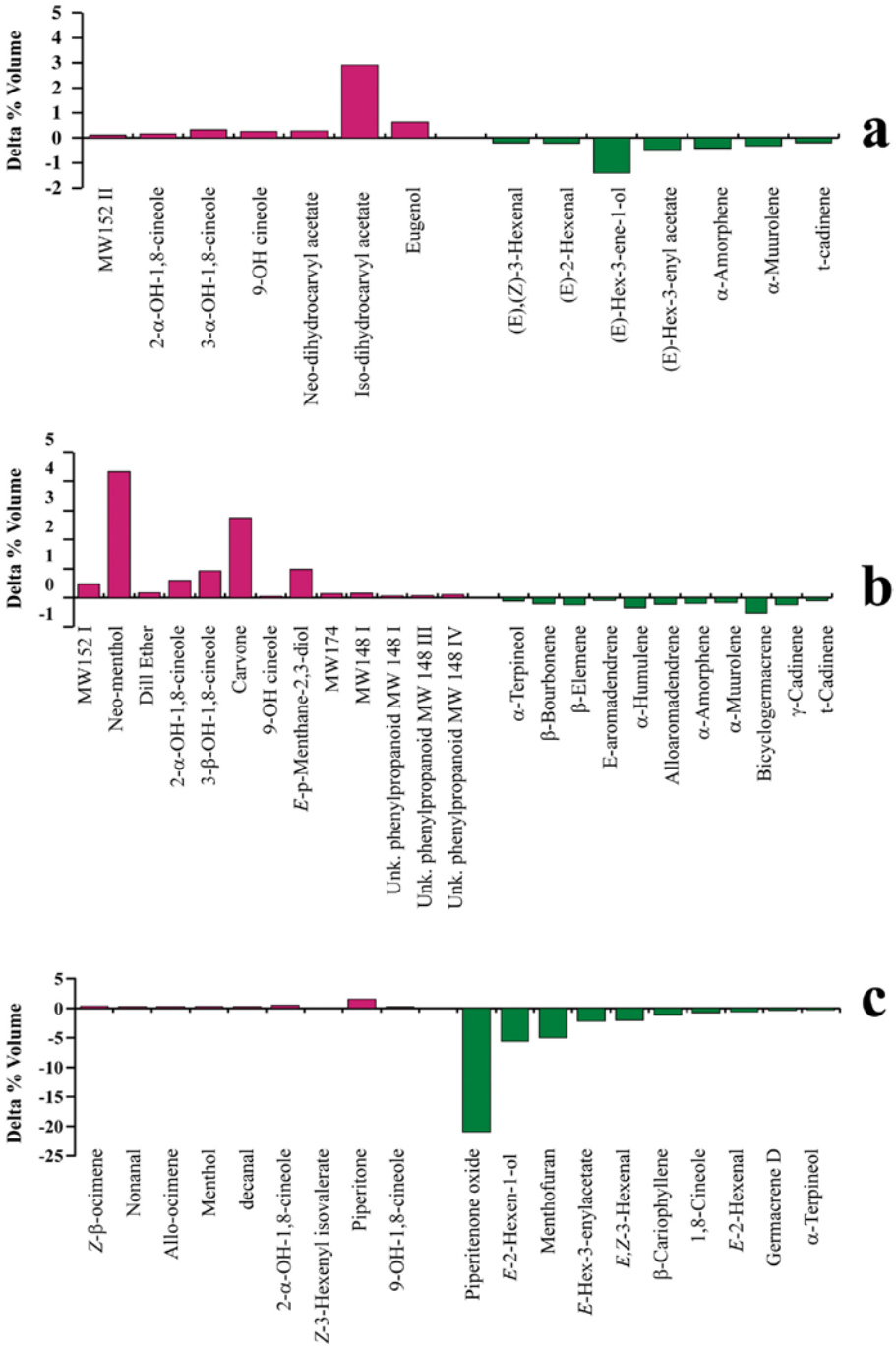
a
Delta % Volume
5
4
3
2
1
0
-1
-2
MW152 II
2-α-OH-1,8-cineole
3-α-OH-1,8-cineole
9-OH cineole
Neo-dihydrocarvyl acetate
Iso-dihydrocarvyl acetate
Eugenol
(E),(Z)-3-Hexenal
(E)-2-Hexenal
(E)-Hex-3-ene-1-ol
(E)-Hex-3-enyl acetate
α-Amorphene
α-Muurolene
t-cadinene
b
Delta % Volume
5
4
3
2
1
0
-1
MW152 I
Neo-menthol
Dill Ether
2-α-OH-1,8-cineole
3-β-OH-1,8-cineole
Carvone
9-OH cineole
E-p-Menthane-2,3-diol
MW174
MW148 I
Unk. phenylpropanoid MW 148 I
Unk. phenylpropanoid MW 148 III
Unk. phenylpropanoid MW 148 IV
α-Terpineol
β-Bourbonene
β-Elemene
E-aromadendrene
α-Humulene
Alloaromadendrene
α-Amorphene
α-Muurolene
Bicyclogermacrene
γ-Cadinene
t-Cadinene
c
Delta % Volume
5
0
-5
-10
-15
-20
-25
Z-β-ocimene
Nonanal
Allo-ocimene
Menthol
decanal
2-α-OH-1,8-cineole
Z-3-Hexenyl isovalerate
Piperitone
9-OH-1,8-cineole
Piperitenone oxide
E-2-Hexen-1-ol
Menthofuran
E-Hex-3-enylacetate
E,Z-3-Hexenal
β-Cariophyllene
1,8-Cineole
E-2-Hexenal
Germacrene D
α-Terpineol

HS-SPME-GCxGC-qMS volatile metabolite profiling of *Chrysolina herbacea* frass and *Mentha* spp. leaves

Chiara Cordero[1a], Simon Atsbaha Zebelo[2a], Giorgio Gnavi[2], Alessandra Griglione[1], Carlo Bicchi[1], Massimo E. Maffei[2] and Patrizia Rubiolo [1*]

[1] Dipartimento di Scienza e Tecnologia del Farmaco, Università di Torino, Via Pietro Giuria n°9 - 10125 Torino, Italy
[2] Unità di Fisiologia Vegetale, Dipartimento di Biologia Vegetale, Università di Torino, Centro della Innovazione, Via Quarello 11/A, 10135 Torino, Italy

SUPPLEMENTARY DATA

Spectral data of unknown compounds listed in Table 1

Compound 30

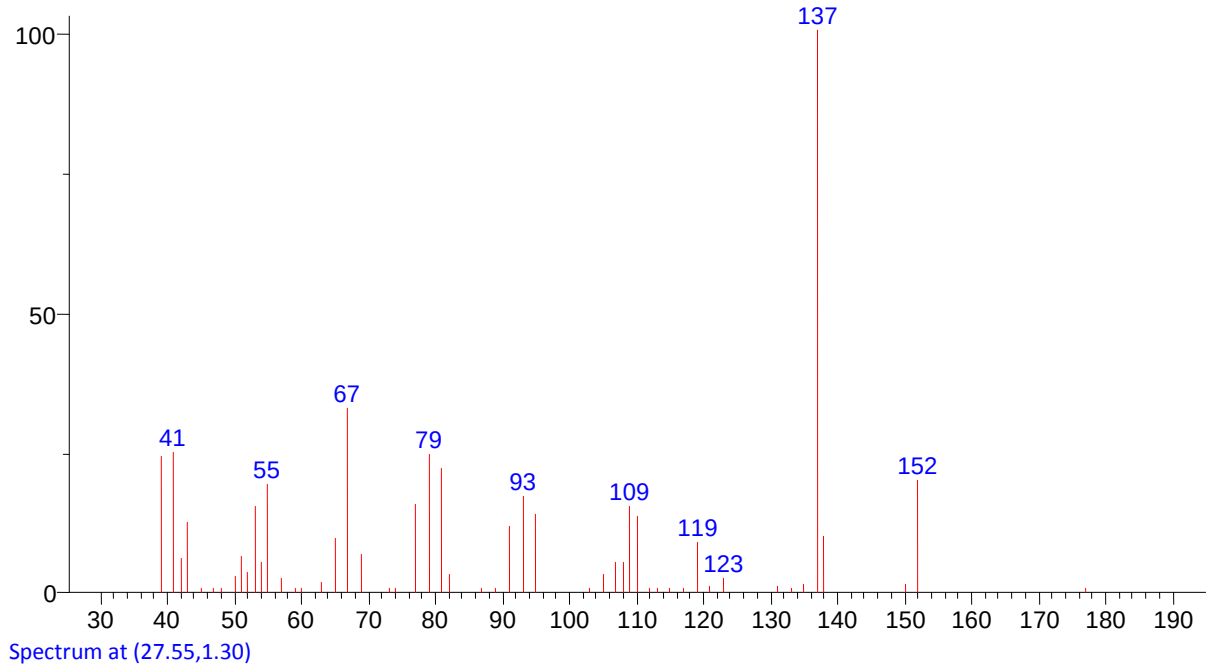

Compound 31

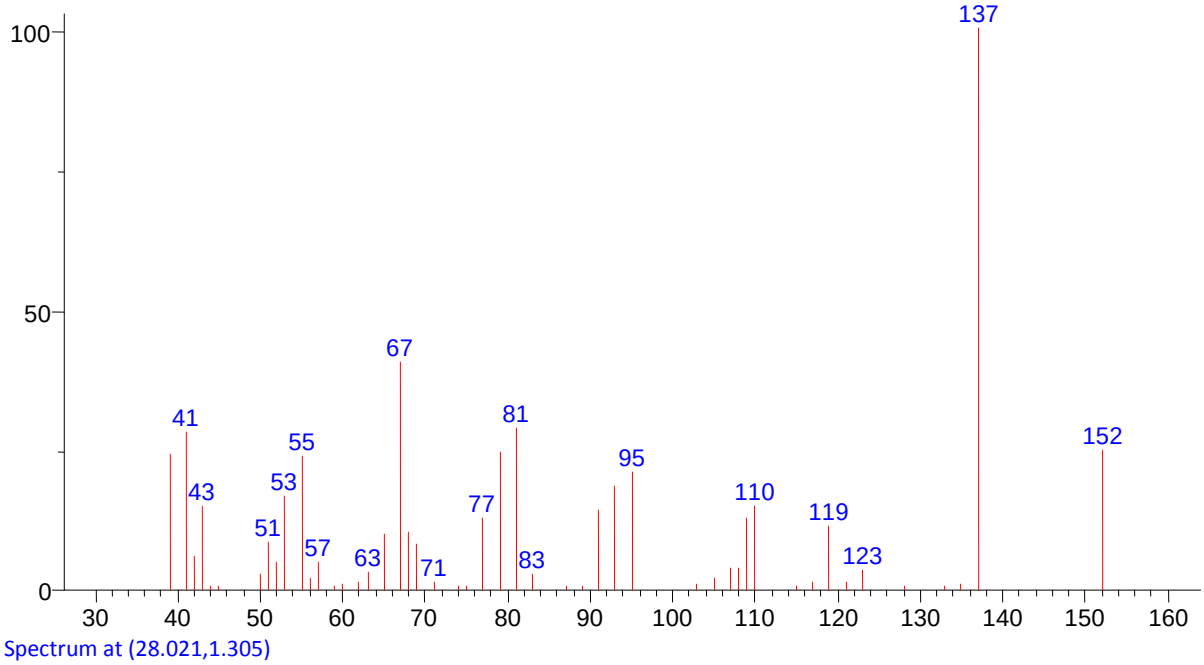

Compound 60

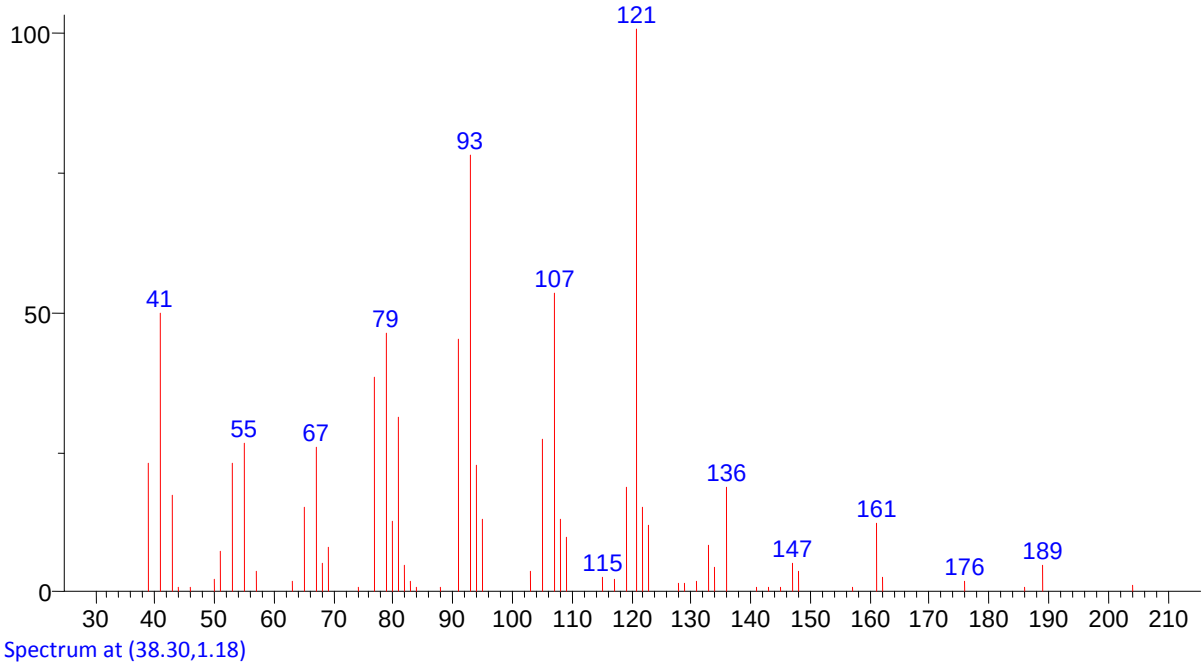

Compound 65

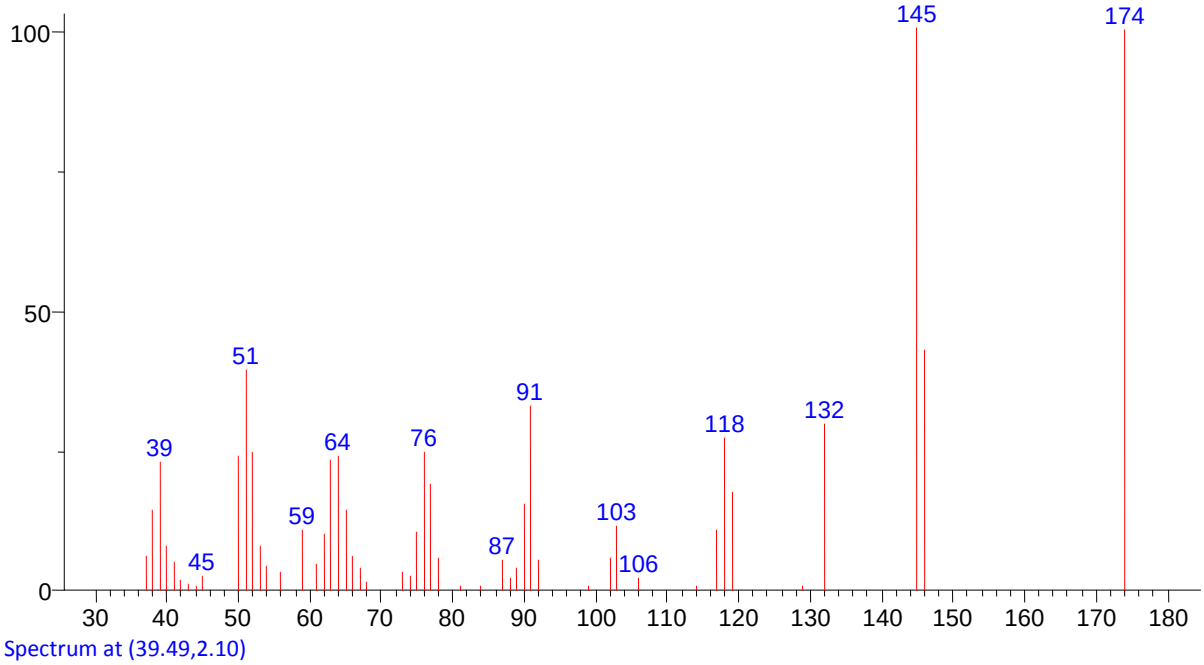

Compound 67

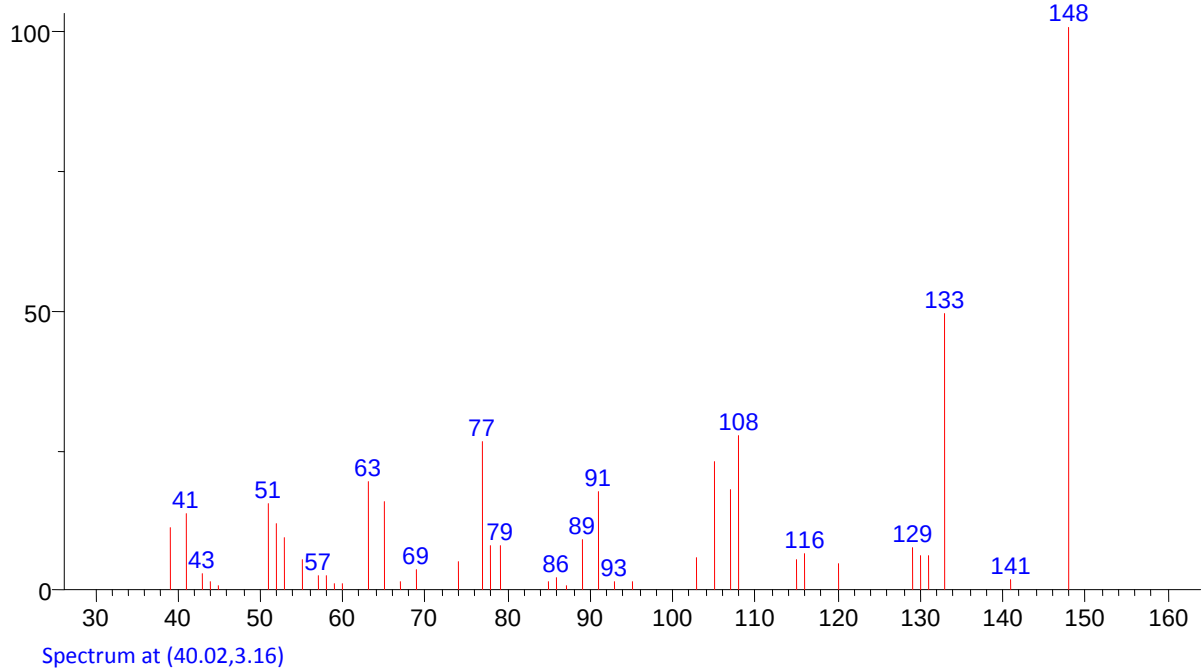

Compound 72

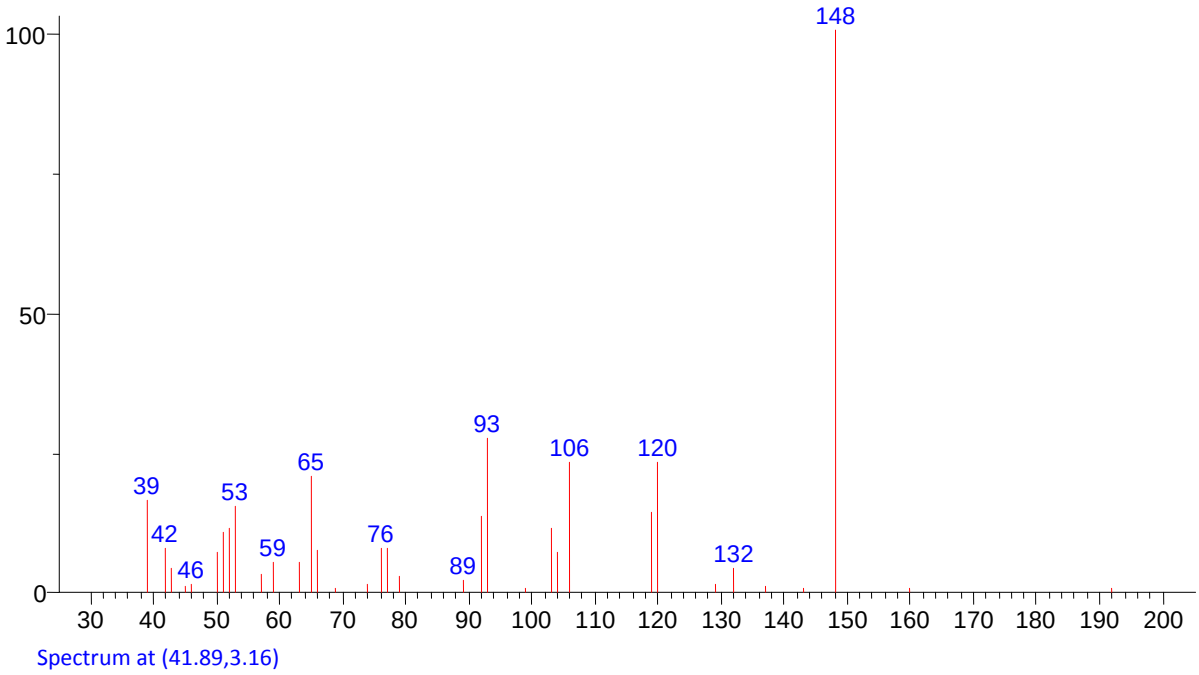

Compound 74

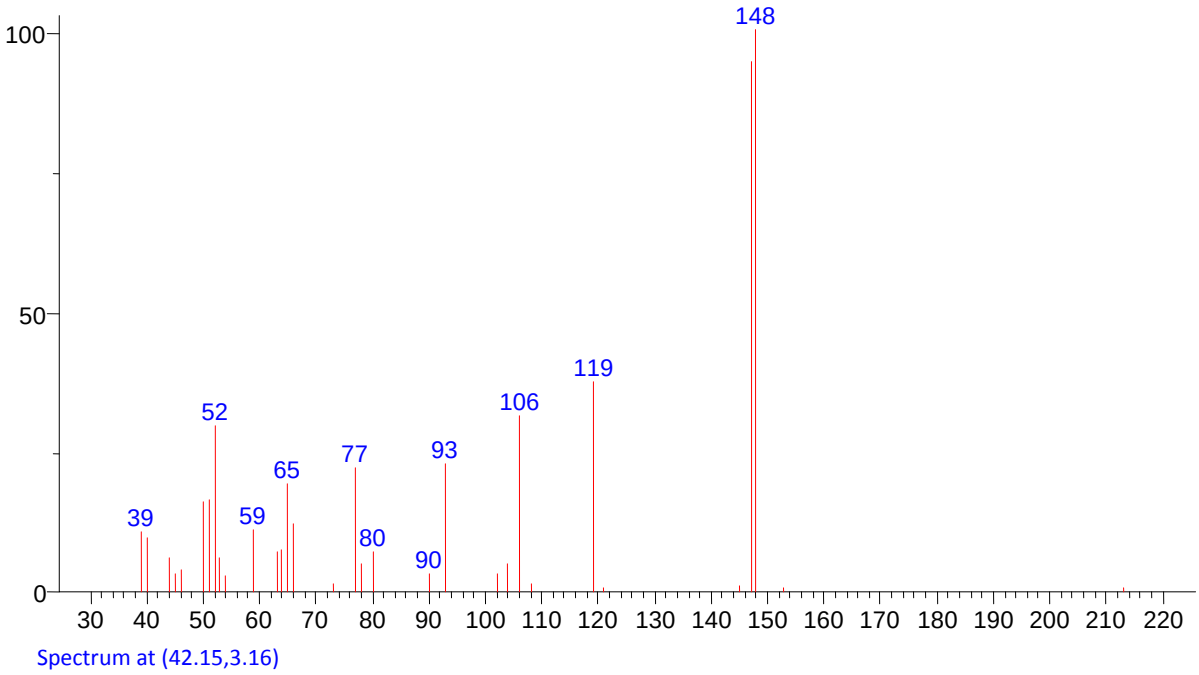

Compound 75

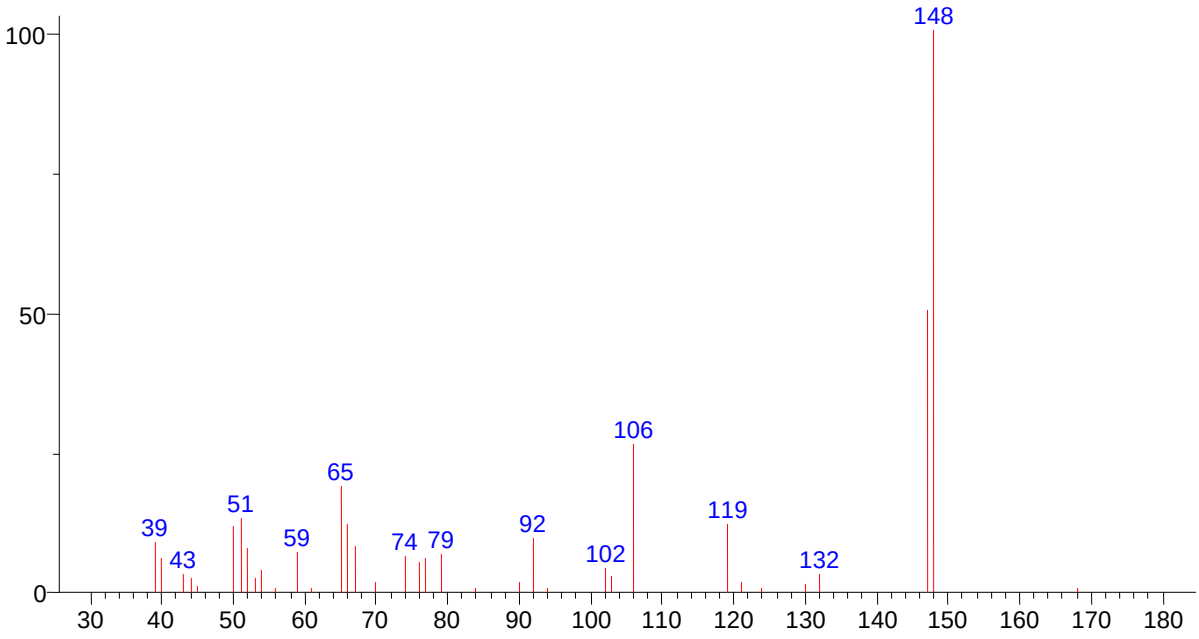
100
50
0
148
106
65
51
39
43
59
74
79
92
102
119
132
30
40
50
60
70
80
90
100
110
120
130
140
150
160
170
180
Spectrum at (42.35,3.32)